Scintigraphic Evaluation of Liver Masses: Cavernous Hepatic Hemangioma

Guest Editor: Abass Alavi
Case Presentation and Discussion: Raymond A. Rubin and Gary R. Lichtenstein

Gastrointestinal Section, Hospital of the University of Pennsylvania, Philadelphia, Pennsylvania

J Nucl Med 1993; 34:849–852

CASE PRESENTATION

A 54-yr-old female was referred for evaluation of a mass in the right lobe of the liver noted on abdominal ultrasound. She had been in her usual state of health until 1 wk prior to admission to this institution when she noted episodic cramping right flank pain. She denied jaundice, pruritus, constitutional symptoms or change in bowel habits. Microhematuria was noted on urinalysis. An intravenous pyelogram demonstrated a nonobstructing ureteral stone. While the kidneys appeared normal on abdominal ultrasound, a large complex echogenic mass of the right lobe of the liver was detected.

The patient's medical history was notable only for a total abdominal hysterectomy with bilateral salpingo-oophorectomy performed for uterine leiomyomata. She took no medications. She neither drank alcohol nor used intravenous drugs. There was no family history of liver disease. Physical examination revealed a healthy appearing black female without stigmata of chronic liver disease. There were numerous rubbery cervical and submandibular lymph nodes as well as a 5–6-cm multinodular goiter. By percussion, the liver span was 10 cm in the mid-clavicular line. No tenderness, hepatic or abdominal masses, splenomegaly or ascites were noted. The remainder of the examination was within normal limits.

Laboratory values revealed normocytic anemia with hyperlobulated polymorphonuclear leukocytes on peripheral blood smear. Liver function tests, electrolytes, coagulation studies, α-fetoprotein and the remainder of the complete blood count were within normal limits. Serum gastrin was 262 pg/ml (nl 0–100), cyanocobalamin level was <100 ng/liter (nl 200–1200) and anti-parietal cell anti-thyroid microsomal antibodies were markedly positive, consistent with the diagnoses of pernicious anemia and Hashimoto's thyroiditis.

Esophagogastroduodenoscopy demonstrated achlorhydria and several hyperplastic gastric polyps. Biopsy of thickened folds within the gastric fundus revealed a moderately dense infiltrate of small, slightly irregular mature lymphocytes involving the mucosa and extending through the muscularis. Although immunohistochemistry and gene rearrangement studies were not diagnostic, these findings raised the concern for a possible low-grade non-Hodgkin's lymphoma. Lymph node and thyroid biopsies demonstrated nonspecific inflammation.

The initial differential diagnosis for the hepatic mass included primary hepatic neoplasm, metastatic disease or cavernous hemangioma. Magnetic resonance imaging (MRI) with intravenous gadolinium-DTPA demonstrated an 8-cm lesion in the posterior segment of the right lobe of the liver, which was dark on T1 and bright on T2 images (Fig. 1). The borders of the mass were slightly irregular. The first postcontrast image was not obtained until 4 min after gadolinium was injected. The mass did not enhance peripherally. The enhancement pattern decreased on the more delayed images. Whereas this was interpreted to be consistent with hemangioma, adenoma or focal nodular hyperplasia, hepatocellular carcinoma or hypervascular endocrine tumor were not ruled out.

Images of the liver were obtained following the intravenous administration of 20 mCi of ^{99m}Tc-labeled red blood cells (RBCs). Sequential images revealed a relatively photopenic area in the inferoposterior aspect of the right lobe of the liver (Fig. 2). Delayed images subsequently demonstrated increased activity within the lesion. SPECT imaging confirmed the presence of a focal area of increased activity (Fig. 3). These findings were believed to be diagnostic of hepatic cavernous hemangioma (HCH).

DISCUSSION

Hepatic cavernous hemangioma is the most common benign neoplasm of the liver (*1*). Focal lesions suggestive of HCH are often incidentally discovered on sonography, CT or radionuclide scintigraphy. Distinguishing HCH from other hepatic masses, especially primary or meta-

Received Aug. 26, 1992; revision accepted Sept. 15, 1992.
For correspondence or reprints contact: Gary R. Lichtenstein, MD, Hospital of the University of Pennsylvania, Gastrointestinal Section, 3rd Floor, Dulles Building, 3400 Spruce St., Philadelphia, PA 19104-4283.

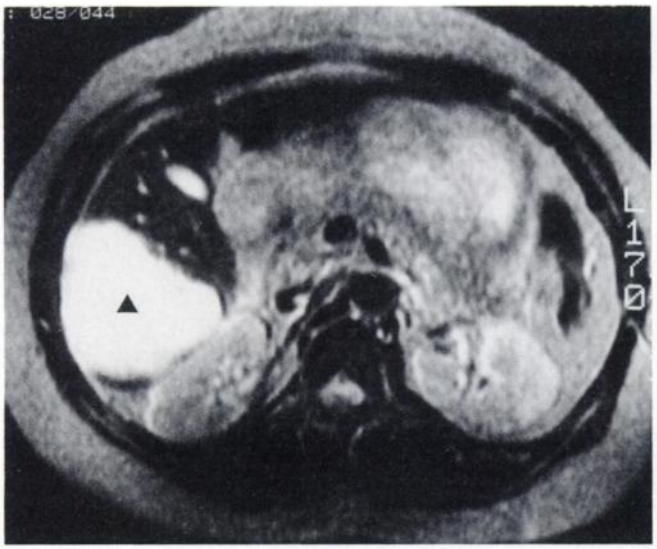

FIGURE 1. T2-weighted transverse magnetic resonance image of the abdomen demonstrates an 8-cm high intensity mass (triangle) in the posterior aspect of the right lobe of the liver.

static malignancy, is a relatively common clinical challenge. As this particular case illustrates, specific imaging studies may be diagnostic of HCH. The appropriate utilization of available radiologic techniques may expedite establishing the specific diagnosis of HCH and avert expensive and potentially harmful testing.

As demonstrated by this case, HCH is generally detected incidentally during radiologic studies, laparotomy or autopsy. It is found in all age groups and 60%–80% are seen in females (*2*), in whom estrogens may contribute to the growth of these lesions (*1*). Similar to hepatic adenomas, the majority of HCHs are located in the right lobe of the liver (*3,4*). Lesions are typically solitary, although 11%–33% of the time they are multiple. The majority of patients with HCH have normal liver function tests and are asymptomatic. Patients with "giant" HCH (exceeding 4 cm in size) more commonly describe abdominal fullness, belching, weight loss and pain. Morbidity may be attributed to bleeding, infarction, necrosis and, rarely, rupture (Table 1).

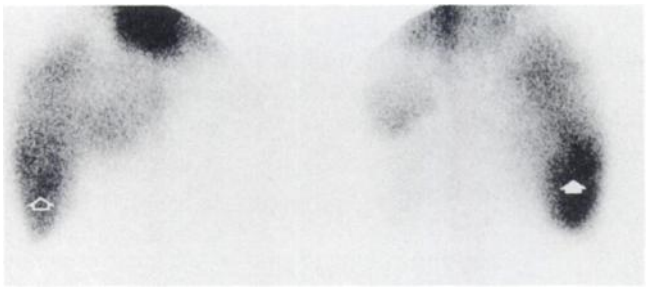

FIGURE 2. Anterior (Left) and posterior (Right) planar blood-pool images demonstrate intense concentration (arrows) of ^{99m}Tc-labeled RBCs in the inferoposterior aspect of the right lobe of the liver.

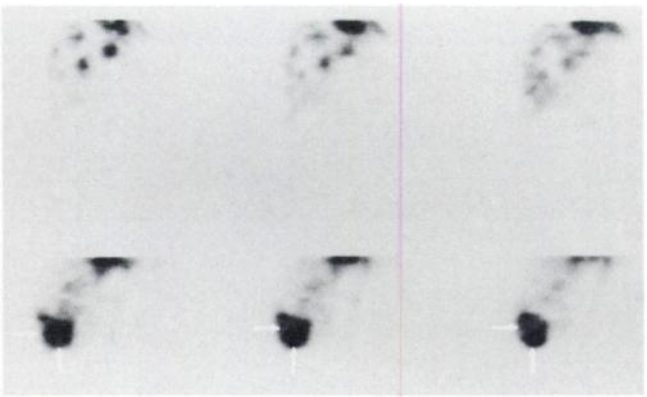

FIGURE 3. Coronal SPECT images of the liver demonstrate intense concentration of activity in the inferoposterior aspect of the right lobe of the liver. With SPECT imaging, the lesion (between arrows) is clearly distinguished from the adjacent normal liver.

Pathologically, HCH consists of large, thin-walled, blood-filled vascular spaces lined by flattened epithelium and separated by fibrous septae (*1*). In giant hemangiomas, the increased endothelial surface may sequester platelets, resulting in a thrombocytopenic coagulopathy known as the Kassabach-Meritt syndrome (*5*).

Imaging of Hemangiomas

Radionuclide Scintigraphy. The routine ^{99m}Tc-sulfur colloid liver scan offers little help in differentiating HCH from other space-occupying lesions of the liver (*3*). On the liver-spleen scan, HCH typically appears as a nonspecific cold defect in an otherwise normal liver (*4*).

Serial planar blood-pool scintigraphy with [^{99m}Tc]pertechnetate labeled RBCs is very specific, if not diagnostic, for the noninvasive diagnosis of hemangioma. Sluggish blood flow through the tortuous vascular pathways produces a "perfusion/blood-pool mismatch" of initial hypoperfusion with gradually increasing RBC accumulation on serial delayed imaging, which peaks within 30 to 50 min after injection (*3,6,7*).

Isolated cases of HCH have been reported in which increased arterial blood supply demonstrated not only red cell accumulation in the delayed images, but also on early perfusion and blood-pool images (*8*). Alternatively, some hemangiomas will be largely fibrotic and will not show the expected increased blood pool (*6*).

The specificity and positive predictive value of labeled RBC scanning approaches 100% (*9,10*). No lesions other than HCHs have been described as showing red cell

TABLE 1
Clinicopathologic Classification of Cavernous Hemangioma

1. Solitary or multiple without symptoms
2. Solitary or multiple with symptoms
3. Giant hemangiomas
4. Hemangiomatosis, exclusive of hepatic involvement
5. Hemangiomatosis, hepatic and extrahepatic involvement

accumulation on delayed images, except for three reported cases of hepatocellular carcinomas (HCCs), a reported case of an angiosarcoma and possibly hypervascular metastases (*7,11*).

While planar studies may not demonstrate small (<3 cm) hemangiomas, smaller lesions may be detected with the use of SPECT (*12–15*). SPECT is also superior to planar imaging for detecting hemangiomas adjacent to the spleen and kidney (*16*). Since labeled RBC activity persists in the heart and major intrahepatic blood vessels on delayed SPECT blood-pool images, it may be difficult to identify small hemangiomas when they are adjacent to these structures (*9*). Large (>4 cm) cavernous hemangiomas have been missed by both planar and SPECT ^{99m}Tc-RBC imaging (*14*). False-negative labeled RBC SPECT is noted when hemangiomas are complicated by thrombosis or fibrosis (*17*).

With the use of a three-headed high-resolution dedicated SPECT system, HCHs as small as 0.5 cm have been detected with serial blood-pool scintigraphy (*16*). When lesions are larger than 1.4 cm, this method has a sensitivity of 100% (*16*). In vitro labeling instead of in vivo labeling of RBCs may improve SPECT's sensitivity for detecting small and/or thrombosed HCHs (*17,18*).

Ultrasonography (US). On US, 50%–60% of hemangiomas demonstrate a homogenous, hyperechoic pattern with well defined margins (*19*). Hepatic adenomas, focal nodular hyperplasia, HCC and solitary hepatic metastases may also appear as solitary, homogenous, hyperechoic masses. Large HCHs may show atypical complex sonographic patterns with areas of mixed echogenicity (*19*). Ultrasound is not, however, the diagnostic imaging modality of choice because of the variable sonographic appearance of HCH.

Computerized Axial Tomography (CT). The finding of small (<1 cm) areas of globular enhancement on dynamic bolus CT, which is analogous to areas of puddling of contrast material seen on angiography and dynamic contrast-enhanced MRI, is suggestive of HCH (*20*). The sensitivity of this finding, especially for small HCHs, has not been determined. Hemangiomas larger than 3 cm can be diagnosed on single-level dynamic, sequential CT scanning, in which the liver is scanned before and then repeatedly after the injection of contrast. "Diagnostic" criteria for use of this technique include a hypodense lesion on unenhanced images, peripheral enhancement during dynamic bolus infusion of contrast and centripetal filling to complete isodensity or hyperdensity on delayed scans obtained up to 60 min after contrast infusion. Only 55%–62% of HCHs satisfy this triad of findings (*21*).

HCC and metastases may also manifest as hypodense lesions that enhance centripetally on CT. When patients with known malignancies are examined with dynamic CT scanning, 86% of the hepatic lesions fulfilling these criteria prove to be HCH (*22*). Small HCHs (<2 cm) may be hard to scan dynamically because of respiration artifact and/or volume averaging with normal liver tissue.

Magnetic Resonance Imaging. MRI has emerged as an accurate and safe, though expensive, method for diagnosing hemangiomas (*23*). HCH usually appears as a smooth, homogenous mass of high signal intensity on T2-weighted images (*24*). Other features, such as a lobulated contour and peripheral location may be helpful in the MR diagnosis of HCH (*25*). HCHs larger than 4 cm may demonstrate atypical features, such as an irregular outline or inhomogenous internal architecture (*26*). MRI has greater sensitivity than labeled RBC SPECT scanning in detecting small (<2–2.5 cm) HCHs. It is also superior in identifying lesions adjacent to the heart and major intrahepatic vessels (*9*).

The ability of MRI to distinguish HCH from metastases is dependent in part on the histology of the primary tumor. Hypervascular metastases from endocrine tumors, sarcomas and adenocarcinomas of the lung, pancreas and uterus have been confused with HCH since they may also appear as homogenous, hyperintense lesions on T2-weighted images (*9,26*).

Modifications of MRI which may facilitate differentiation of HCH from metastases or small HCCs have included ultrafast imaging, alternative pulse sequence selection and dynamic contrast-enhanced imaging (*27–29*). Clinical experience with these techniques for imaging hypervascular metastases has been limited.

Angiography. Angiography traditionally has been the gold standard for diagnosing HCHs. It is, however, invasive and expensive. Because other imaging techniques have been introduced and refined, angiography is often reserved for diagnostically equivocal cases or preoperative assessment.

Specific and diagnostic features of hemangioma on angiography include rapid filling of vascular spaces with contrast material in the arterial phase and persistent opacification in the venous phase. Large, blood-filled spaces fill with contrast several seconds after injection, thus producing a "cotton wool" appearance (*6*). Unlike HCC or metastases, there is no arteriovenous shunting or neovascularity. Normal arteriograms can be encountered in very small hemangiomas. For larger lesions with extensive fibrosis or thrombosis, arteriography may be nondiagnostic (*30*).

SUMMARY

Hepatic cavernous hemangioma must be included in the differential diagnosis of any hepatic solid mass. It is the second most common neoplasm of the liver, following intrahepatic metastases. With the exception of giant or symptomatic HCH, it does not require specific intervention. The ability to diagnose HCH radiologically (Table 2) has significant clinical importance.

When confronted with clinical data and a preliminary radiologic study suggestive of HCH, serial planar blood-pool scintigraphy (with SPECT if the lesion is <3–4 cm) should probably be the initial diagnostic examination. In

TABLE 2
Characteristic Appearance of HCH in Different Imaging Modalities

Imaging technique	Radiologic findings
Serial blood-pool scintigraphy	"Perfusion/blood-pool mismatch" of initial hypoperfusion with gradually increasing RBC accumulation on serial delayed images.
Ultrasound	Homogenous hyperechoic pattern with well defined margins.
Dynamic CT	Hypodense lesion on unenhanced images, peripheral enhancement during contrast infusion and centripetal filling to isodensity or hyperdensity on delayed images.
MRI	Smooth, homogenous mass of high signal intensity on T2-weighted images.
Angiography	Rapid filling of vascular spaces with contrast in the arterial phase and persistent opacification into the venous phase.

comparison to MRI, it is safer, less expensive and easier for some patients to tolerate. For small, deep seated lesions or those adjacent to the heart or large vessels, MRI is the preferred test. Dynamic CT is probably most useful in patients with normal renal function in whom optimal imaging of the extrahepatic abdomen is desired.

If the etiology of an incidental hepatic mass suspected to be an HCH is still not evident after these studies, angiography or biopsy are the remaining options. As described, angiography is sensitive and relatively specific for HCH. Although percutaneous biopsy may be associated with increased risk of bleeding, fine-needle biopsy has been shown to be safe for hemangiomas. However, fine-needle biopsy is more useful for confirming a suspected malignancy than for actually diagnosing hemangioma (*31*).

REFERENCES

1. Ishak KG, Rabin L. Benign tumors of the liver. *Med Clin North Am* 1975;59:995–1013.
2. Tahagi H. Diagnosis and management of cavernous hemangioma of the liver. *Semin Surg Oncol* 1985;1:12–22.
3. Prakash R, Jena A, Behari V, et al. Technetium-99m red blood cell scintigraphy in diagnosis of hepatic hemangioma. *Clin Nucl Med* 1987;12: 235–237.
4. Moinuddin M, Allison JR, Montgomery JH, et al. Scintigraphic diagnosis of hepatic hemangioma: its role in the management of hepatic mass lesions. *AJR* 1985;145:223–228.
5. Kassabach HH, Merritt KF. Cavernous hemangioma with extensive purpura. Report of a case. *Am J Dis Child* 1940;59:1063–1070.
6. Brant WE, Floyd JL, Jackson DE, et al. The radiological evaluation of hepatic cavernous hemangioma. *JAMA* 1987;257:2471–2474.
7. Drane WE. Nuclear medicine techniques for the liver and biliary system. *Radiol Clin North Am* 1991;29:1129–1151.
8. Larcos G, Farlow DC, Grunewald SM, et al. Atypical appearance of a hepatic hemangioma with technetium-99m-red blood cell scintigraphy. *J Nucl Med* 1989;30:1885–1888.
9. Birnbaum BA, Weinreb JC, Megibow AJ, et al. Definitive diagnosis of hepatic hemangiomas: MR imaging versus Tc-99m-labeled-red blood cell SPECT. *Radiology* 1990;1776:95–101.
10. Kudo M, Ikekubo K, Yamamoto K, et al. Distinction between hemangioma of the liver and hepatocellular carcinoma: value of labeled RBC-SPECT scanning. *AJR* 1989;152:977–983.
11. Ginsberg F, Slavin JD, Spencer RP. Hepatic angiosarcoma: mimicking of hemangioma on three-phase technetium-99m-red blood cell scintigraphy. *J Nucl Med* 1986;27:1861–1863.
12. Brodsky RI, Friedman AC, Maurer AH, et al. Hepatic cavernous hemangioma: diagnosis with ^{99m}Tc-labeled red cells and SPECT. *AJR* 1987;148: 125–129.
13. Tumeh SS, Benson C, Nagel JS, et al. Cavernous hemangioma of the liver: detection with single photon emission computed tomography. *Radiology* 1987;164:353–356.
14. Intenzo C, Kim S, Madsen M, et al. Planar and SPECT Tc-99m red blood cell imaging in hepatic cavernous hemangiomas and other hepatic lesions. *Clin Nucl Med* 1988;13:237–240.
15. Malik MH. Blood-pool SPECT and planar imaging in hepatic hemangioma. *Clin Nucl Med* 1987;12:543–547.
16. Zeissman HA, Silverman PM, Patterson J, et al. Improved detection of small cavernous hemangiomas of the liver with high-resolution three-headed SPECT. *J Nucl Med* 1991;32:2086–2091.
17. Rabinowitz SA, McKusick KA, Strauss HW. Technetium-99m red blood cell scintigraphy in evaluating focal liver lesions. *AJR* 1984;143:63–68.
18. Floyd JL, Jackson DE. In vivo versus in vitro labeling of red blood cells in hepatic cavernous hemangioma [letter]. *J Nucl Med* 1986;27:1940–1941.
19. Prakash R, Gupta RK, Narayanan R, et al. Technetium-99m radiocolloid scintigraphy, planar, and SPECT red blood cell imaging and ultrasonography in diagnosis of hepatic hemangioma. *Austr Radiol* 1989;33:237–244.
20. Quinn SF, Benjamin GG. Hepatic cavernous hemangioma: simple diagnostic sign with dynamic bolus CT. *Radiology* 1992;182:545–548.
21. Freeny PC, Marks WM. Hepatic hemangioma: dynamic bolus CT. *AJR* 1986;147:711–719.
22. Freeny PC, Marks WM. Patterns of contrast enhancement of benign and malignant hepatic neoplasms during bolus dynamic and delayed CT. *Radiology* 1988;155:417–420.
23. Stark DD, Felder RC, Wittenberg J, et al. Magnetic resonance imaging of cavernous hemangioma of the liver. *AJR* 1985;145:213–222.
24. Sigal R, Lanier A, Atlan H, et al. Nuclear magnetic resonance imaging of liver hemangiomas. *J Nucl Med* 1985;26:1117–1122.
25. Ros PR, Lubbers PR, Olmsted WW, et al. Hemangioma of the liver: heterogenous appearance on T2-weighted images. *AJR* 1987;149:1167–1170.
26. Li KC, Glazer GM, Quint LE, et al. Distinction of hepatic cavernous hemangioma from hepatic metastases with MR imaging. *Radiology* 1988; 169:409–415.
27. Goldberg MA, Saini S, Hahn PF, et al. Differentiation between hemangiomas and metastases of the liver with ultrafast MR imaging: preliminary results with T2 calculations. *AJR* 1991;157:727–730.
28. Hamm B, Fischer E, Taupitz M. Differentiation of hepatic hemangiomas from metastases by dynamic contrast-enhanced MR imaging. *J Comput Assist Tomog* 1990;24:205–216.
29. Choi BI, Han MC, Kim C. Small hepatocellular carcinoma versus small cavernous hemangioma: differentiation with MR imaging at 2.0 T. *Radiology* 1990;176:103–106.
30. Davis WD, Ferrante WA, Tutton RH, et al. Hepatic hemangioma with normal angiograms. *JAMA* 1990;263:983–986.
31. Solbiati L, Libraghi T, DePra L, et al. Fine-needle biopsy of hepatic hemangioma with sonographic guidance. *AJR* 1985;144:471–474.